

The promise of dawn: microalgae photoacclimation as an optimal control problem of resource allocation

F. Mairet, T erence Bayen

► **To cite this version:**

F. Mairet, T erence Bayen. The promise of dawn: microalgae photoacclimation as an optimal control problem of resource allocation. 2020. hal-02925993

HAL Id: hal-02925993

<https://hal-univ-avignon.archives-ouvertes.fr/hal-02925993>

Preprint submitted on 31 Aug 2020

HAL is a multi-disciplinary open access archive for the deposit and dissemination of scientific research documents, whether they are published or not. The documents may come from teaching and research institutions in France or abroad, or from public or private research centers.

L'archive ouverte pluridisciplinaire **HAL**, est destin ee au d ep ot et  a la diffusion de documents scientifiques de niveau recherche, publi es ou non,  emanant des  tablissements d'enseignement et de recherche franais ou  trangers, des laboratoires publics ou priv es.

The promise of dawn: microalgae photoacclimation as an optimal control problem of resource allocation

Francis Mairet*, T erence Bayen†

August 31, 2020

Abstract

Photosynthetic microorganisms are known to adjust their photosynthetic capacity according to light intensity. This so-called photoacclimation process may correspond at equilibrium to the optimal behavior in order to maximize growth. But its dynamics under varying condition remains less understood. To tackle this problem, we propose here a resource allocation model, at coarse-grained, to represent microalgae growth and photoacclimation. Using the Pontryagin maximum principle and numerical simulations, we determine the optimal strategy of resource allocation in order to optimize microalgal growth rate over a time horizon. We show that, after a transient, the optimal trajectory approaches the optimal steady state, a behavior known as the turnpike property. Then, the model is fitted with experimental data, resulting in a bi-level optimization problem which is solved numerically. The fitted trajectory represents well a *Dunaliella tertiolecta* culture facing a light down-shift. Finally, we compute the optimal trajectory under day/night cycle and show that the synthesis of the photosynthetic apparatus starts a few hours before dawn. This anticipatory behavior has actually been observed both in the laboratory and in the field. This shows the algal predictive capacity and the interest of our method which predicts this phenomenon.

Keywords: Turnpike, Bi-level optimization, Microalgal growth model, Photosynthetic apparatus, Anticipatory behavior.

1 Introduction

Microalgae are key players in the ocean [11], and they also represent a promising resource for various markets (feed, health, etc) [32]. These microorganisms adjust their photosynthetic apparatus according to the light they received: *e.g.*, if light is in excess, the photosynthetic apparatus will decrease [21]. This so-called photoacclimation process is an important factor to consider when estimating net primary production in the ocean from satellite chlorophyll measurements [16], or when optimizing microalgal production given the interplay between self-shading and light limitation [4, 9].

Mathematical models have been proposed to understand and predict microalgal photoacclimation. They can be divided into two types: empirical models, mainly based on experimental observations (*e.g.*, [13, 12, 4, 27, 33]), and optimality-based models. The latter type relies on the hypothesis, widespread for predictive models in biology, that evolution has resulted in organisms having optimal performances [35]. Microbial growth can thus be formalized as an optimization problem, where resources should be allocated between different sectors in order to maximize the growth rate for exemple. In this framework, photoacclimation models based on static optimization have been proposed by [31, 2, 14, 19, 10, 43]. These models correctly represent photoacclimation in a constant environment. Nonetheless, light supply is always changing, because of the sunpath, the presence of clouds, the position of the cell in the water column, etc. In this context, [37] have determined a fixed resource allocation which maximizes the growth over a time window under light fluctuations. However, this study still neglects photoacclimation dynamics. Instantaneous optimization has been proposed to represent photoacclimation under variable conditions [42]. That is, at each instant, the chlorophyll content is adjusted so as to maximize instantaneous growth. It appears that such a strategy is not necessarily optimal over the

*Ifremer, Physiology and Biotechnology of Algae laboratory, rue de l'Île d'Yeu, 44311 Nantes, France
francis.mairet@ifremer.fr

†Avignon Universit e, Laboratoire de Math ematiques d'Avignon (EA 2151) F-84018 France.
terence.bayen@univ-avignon.fr)

long term. Generally, one can determine a strategy to maximize growth over a time window. This can be formalized as an optimal control problem, as proposed for example to represent bacterial growth [28, 41, 15]. Concerning photosynthetic microorganisms, to the best of our knowledge, resource allocation optimization over a time window has been tackled only by [8] and [30], focusing on carbon storage over a day-night cycle (and not photoacclimation).

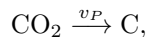
Here a coarse-grained model is proposed to represent microalgae growth and photoacclimation as a resource allocation problem. We first determine the optimal allocation strategy in static conditions, resulting in the classic photoacclimation relationship: the more the light increases, the more the photosynthetic apparatus decreases. Then, we determine the optimal allocation strategy under dynamic conditions, when microalgae face a light shift. Using optimal control theory (Pontryagin's Principle) and numerical simulations (direct methods), we show that the optimal trajectory corresponds to a turnpike, *i.e.*, to quickly adjust the allocation close to the optimal steady state. Then, following our preliminary work [22], a parameter estimation method - leading to a bi-level optimization problem - is proposed and carried out. This results in a first proof of concept of how to calibrate dynamic resource allocation model. Finally, optimal allocation strategy under day/night cycles is determined numerically. This reveals that the synthesis of the photosynthetic apparatus begins a few hours before dawn. This behavior is actually observed in several laboratory and field studies [44, 20, 18], revealing the algal anticipation capacity.

2 Model development

A coarse-grained model of microalgae growth and photoacclimation is proposed, inspired by the works of [31, 15].

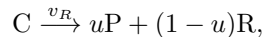
2.1 Biochemical reactions

The model is based on two macroreactions, represented in Figure 1. First, CO_2 is fixed to produce small carbon precursors C (in g):



where v_P corresponds to the photosynthetic rate (in g/(g biomass·d)).

The second reaction corresponds to the synthesis of macromolecules, divided into two sectors: the photosynthetic apparatus, including the photosystems and the enzymes of the Calvin cycles P (in g) and the gene expression machinery (mainly the ribosomes) R (in g):



where v_R (in g/(g biomass·d)) corresponds to the rates of macromolecule synthesis, and $u \in [0, 1]$ is the allocation variable representing the part of the flux going to the synthesis of the photosynthetic apparatus. Considering biomass $B = C + P + R$, a mass balance gives the following dynamics:

$$\begin{cases} \frac{dC}{dt} = v_P B - v_R B, \\ \frac{dP}{dt} = u v_R B, \\ \frac{dR}{dt} = (1 - u) v_R B, \\ \frac{dB}{dt} = v_P B. \end{cases}$$

Now denoting in lowercase the mass fractions (in g/g biomass), *i.e.*, $c = C/B$, $p = P/B$, and $r = R/B$, we finally get

$$\begin{cases} \frac{dc}{dt} = \frac{1}{B} \frac{dC}{dt} - \frac{C}{B^2} \frac{dB}{dt} = v_P(1 - c) - v_R, \\ \frac{dp}{dt} = \frac{1}{B} \frac{dP}{dt} - \frac{P}{B^2} \frac{dB}{dt} = u v_R - p v_P, \\ \frac{dr}{dt} = \frac{1}{B} \frac{dR}{dt} - \frac{R}{B^2} \frac{dB}{dt} = (1 - u) v_R - r v_P. \end{cases}$$

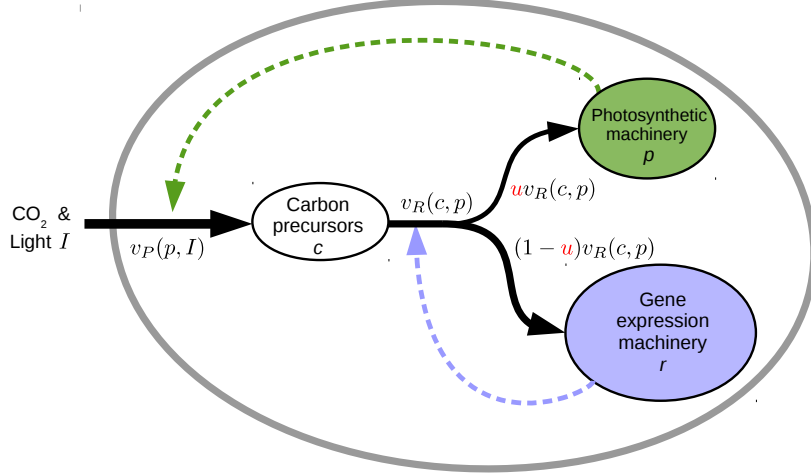


Figure 1: Scheme of the coarse-grained model to represent photoacclimation in microalgae. We assume that microalgae maximize their growth rate by adjusting the resources allocated to the photosynthetic apparatus (through the allocation variable $u \in [0, 1]$).

2.2 Reaction rates

For the kinetics, we consider that the photosynthetic rate is a function of the photosynthetic apparatus mass fraction and of the light intensity I , i.e., $v_P(p, I)$, with the following assumption

Hypothesis 1. *The function $v_P : [0, 1] \times \mathbb{R}_+ \rightarrow \mathbb{R}_+$ is of class C^2 and satisfies*

- For every $p \in [0, 1]$, $v_P(p, 0) = 0$;
- For every $I > 0$, $v_P(0, I) = 0$;
- For every $I > 0$, the mapping $v_P(\cdot, I)$ is strictly concave increasing over the interval $[0, 1]$.

Typically, Michaelis-Menten's function

$$v_P(p, I) = k_P \frac{pI}{K + pI}, \quad (1)$$

satisfies Hypothesis 1. In this expression, the photosynthetic rate is a function of the product pI , which corresponds to the energy absorbed by the cells. This is in line with mechanistic models of photoacclimation, where the rate depends on the product of the chlorophyll content times the light intensity (see *e.g.*, [13]).

The rate of macromolecule synthesis depends on the mass fractions of carbon precursors and the gene expression machinery. A simple mass action kinetics is considered:

$$v_R(c, r) = k_R c r.$$

2.3 Problem statement

Given that $c + p + r = 1$, one variable can be removed and we finally get:

$$\begin{cases} \frac{dc}{dt} = v_P(p, I)(1 - c) - k_R c(1 - c - p), \\ \frac{dp}{dt} = u k_R c(1 - c - p) - p v_P(p, I). \end{cases} \quad (2)$$

Before formalizing the resource allocation problem, we show that the system (2) satisfies the following invariance property. Let us then introduce the set

$$\Omega := \{(c, p) \in (0, 1) \times (0, 1) ; c + p \leq 1\}.$$

Lemma 1. *The set Ω is invariant by (2).*

Proof. Whenever $c = 0$ (resp. $p = 0$), it is easily seen that $\dot{c} = v_P(p, I) > 0$ (resp. $\dot{p} = u(t)k_R c(1 - c) > 0$), so the positive orthant is invariant. In addition, one has $\dot{c} + \dot{p} = 0$ along $c + p = 1$ so that the line segment $L := \{(c, 1 - c) ; c \in [0, 1]\}$ is also invariant. This ends the proof. \square

Since trajectories of (2) starting in L remain in L , we suppose next that initial conditions belong to the (open) invariant domain:

$$\mathcal{D} := \{(c, p) \in (0, 1) \times (0, 1) ; c + p < 1\}.$$

We assume that microalgae have acquired through evolution optimal strategy, *i.e.*, they regulate their allocation of resources in order to maximize their growth. To represent this behavior, we are interested in maximizing the photosynthetic rate v_P w.r.t. the allocation of macromolecules synthesis u (corresponding to our control) over a given time period. Thus, we consider the admissible control set defined as:

$$\mathcal{U} = \{u : [0, T] \rightarrow [0, 1] ; u \text{ meas.}\},$$

in which $T > 0$ is our given time period. The optimization problem under consideration can be then gathered into:

$$\max_{u(\cdot) \in \mathcal{U}} J(u) := \int_0^T v_P(p(t), I) dt, \quad (\text{P})$$

where $(c(\cdot), p(\cdot))$ is the unique solution of (2) starting at a given point $(c_0, p_0) \in \mathcal{D}$ for a given control $u \in \mathcal{U}$.

3 Optimal allocation at equilibrium

Our first objective is to determine the optimal allocation at equilibrium, for a constant light intensity $I > 0$. This corresponds to the static optimization problem:

$$\max_{u \in [0, 1]} \bar{J}(u) := v_P(p_u, I), \quad (3)$$

where (c_u, p_u) is a steady state of (2) associated with the constant control u and a constant light I , *i.e.*,

$$\begin{aligned} 0 &= v_P(p_u, I)(1 - c_u) - k_R c_u(1 - c_u - p_u), \\ 0 &= u k_R c_u(1 - c_u - p_u) - v_P(p_u, I)p_u. \end{aligned} \quad (4)$$

Lemma 2. *There is a unique solution $u^* \in [0, 1]$ to (3)-(4) satisfying*

$$v_P((u^*)^2, I) = k_R(1 - u^*)^2.$$

In addition, the corresponding steady-state (c^, p^*) of (2) is given by*

$$\begin{aligned} c^* &= 1 - u^*, \\ p^* &= (u^*)^2. \end{aligned} \quad (5)$$

Proof. Let us first show that $u = 0$ and $u = 1$ are not optimal solutions of (3)-(4). If $u = 0$, then either $v_P(p_u, I) = 0$ or $p_u = 0$ implying in both cases that the cost $\bar{J}(u)$ is zero. If now $u = 1$, we obtain $v_P(p_u, I)(1 - c_u - p_u) = 0$ and either $p_u = 0$ or $1 - c_u - p_u = 0$. As previously, we can exclude the case $p_u = 0$. But, if now $1 - c_u - p_u = 0$ (with $p_u \neq 0$), we obtain $v_P(p_u, I)(1 - c_u) = 0$, thus $1 - c_u = 0$ and from (4), we get $p_u = 0$ which is not possible. Hence, $u = 1$ is also not optimal.

Let us go back to Problem (3)-(4). From (4), we obtain that any admissible solution of (4) satisfies $p_u = u(1 - c_u)$. Replacing c_u by its value into the first equation then gives

$$g(p, u) := v_P(p, I) - k_R \left(1 - \frac{p}{u}\right) (1 - u) = 0.$$

Problem (3)-(4) then amounts to maximize $u \mapsto \bar{J}(u)$ over $[0, 1]$. Doing so, we apply the classical Karush-Kuhn-Tucker conditions (KKT). Because $u = 0$ and $u = 1$ are not optimal, we can remove the nonbinding

constraint $u \in [0, 1]$ and take into account one equality constraint $g(p, u) = 0$. Let then $\mathcal{L} := \bar{J} + \lambda g$ the Lagrangian associated with (3)-(4). Let u be a maximum of (3)-(4). Then, the stationarity condition

$$\frac{\partial \mathcal{L}}{\partial u} = 0,$$

gives $p = u^2$, and from the equality constraint $g(p, u) = 0$, we obtain

$$v_P(u^2, I) = k_R(1 - u)^2.$$

Since v_P is increasing with $v_P(0, I) = 0$, this equation has a unique solution in $(0, 1)$. The value of (c^*, p^*) follows. \square

Using for v_P the Michaelis-Menten function given in (1), u^* is the unique solution in $[0, 1]$ of a polynomial equation of degree four:

$$-Ik_R u^4 + 2Ik_R u^3 + (Ik_P - k_R K - Ik_R - k_R K)u^2 + 2k_R K u - k_R K = 0.$$

We can compute this solution as a function of the light intensity. We obtain that the optimal photosynthetic machinery sector at equilibrium p^* is a decreasing function of light intensity I , in line with experimental data of steady-state photoacclimation [21], see Fig. 2. Actually, this pattern has already been predicted by steady-state optimization with similar models (*e.g.*, in [2]).

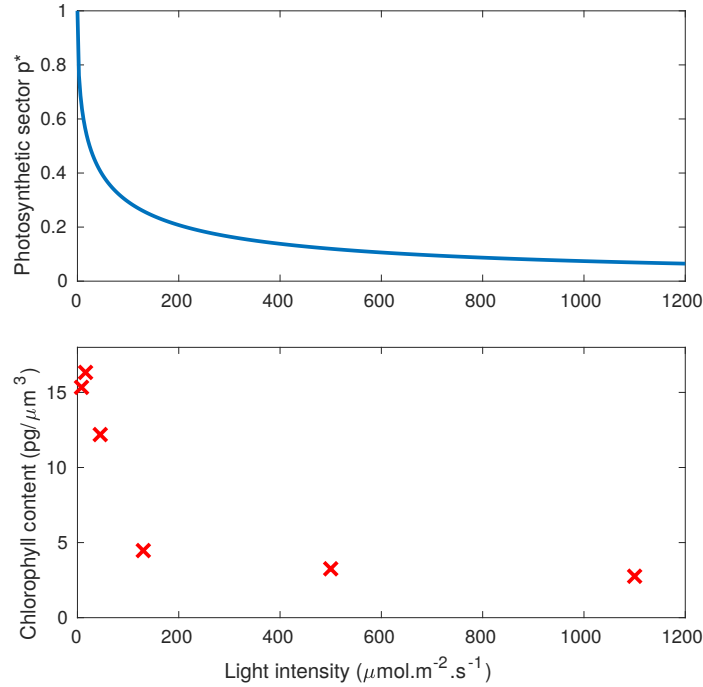


Figure 2: Optimal steady-state allocation for the photosynthetic sector p^* as a function of light intensity (top), see Lemma 2. This pattern corresponds to the photoacclimation phenomena [21], as shown for example by the chlorophyll content measured experimentally for *Dunaliella tertiolecta* [17] (bottom).

The optimal steady-state enjoys the following stability property (of interest whenever perturbations affect the system).

Proposition 1. *The steady-state (c^*, p^*) of (2) associated with the (constant) control $u = u^*$ is locally stable with two negative eigenvalues.*

Proof. At a steady-state (c, p) of (2) associated with a constant control u , the Jacobian matrix is

$$\begin{bmatrix} -v_P(p, I) - k_R(1 - 2c - p) & \frac{\partial v_P}{\partial p}(p, I)(1 - c) + k_R c \\ k_R u(1 - 2c - p) & -k_R u c - \frac{\partial v_P}{\partial p}(p, I)p - v_P(p, I) \end{bmatrix},$$

and, replacing (c, p, u) by the optimal triplet (c^*, p^*, u^*) , it becomes

$$\begin{bmatrix} 0 & \frac{\partial v_P}{\partial p}(p^*, I)u^* + k_R(1 - u^*) \\ -k_R u^*(u^* - 1)^2 & -k_R(1 - u^*) - (u^*)^2 \frac{\partial v_P}{\partial p}(p^*, I) \end{bmatrix}.$$

Since $u^* \in (0, 1)$ and $\frac{\partial v_P}{\partial p} > 0$, the trace and determinant of this matrix are respectively negative and positive which shows that it has exactly two negative eigenvalues. This ends the proof. \square

4 Optimal allocation during a light shift

Our coarse-grained model is now used to study the dynamics of photoacclimation. As a case study, we consider that light intensity is shifted at $t = 0$, and then it remains constant. Our objective is to determine how microalgae can adjust their allocation in order to maximize their growth during the light shift transient. Formally, we thus consider the optimal control problem (P). In the following, $v_P(p, I)$ will be denoted as $v_P(p)$ for sake of simplicity, and v'_P corresponds to its derivative with respect to p .

4.1 Application of the Pontryagin Maximum Principle

Optimal controls are derived using the Pontryagin Maximum Principle (see [29]). Note that the existence of an optimal control is straightforward (due to the linearity of (2) w.r.t. the control), this follows from Fillipov's Theorem [7]. Let us now apply Pontryagin's Principle. Doing so, let $H = H(c, p, \lambda_c, \lambda_p, \lambda^0, u)$ be the Hamiltonian associated with (P) (written as a minimum):

$$H := k_R c(1 - c - p)[u\lambda_p - \lambda_c] + v_P(p)[\lambda_c(1 - c) - \lambda_p p - \lambda^0].$$

If u is an optimal control and $x(\cdot) = (c(\cdot), p(\cdot))$ the associated trajectory, there exists $\lambda^0 \leq 0$ and an absolutely continuous map $\lambda = (\lambda_c, \lambda_p) : [0, T] \rightarrow \mathbb{R}^2$ such that $(\lambda, \lambda^0) \neq 0$ and satisfying the adjoint equation $\dot{\lambda} = -\frac{\partial H}{\partial x}$, that is:

$$\begin{cases} \dot{\lambda}_c &= -k_R(1 - 2c - p)(u\lambda_p - \lambda_c) + v_P(p)\lambda_c, \\ \dot{\lambda}_p &= k_R c(u\lambda_p - \lambda_c) + \lambda_p v_P(p) - v'_P(p)[\lambda_c(1 - c) - \lambda_p p - \lambda^0]. \end{cases} \quad (6)$$

In addition, since the state is free at the terminal time, transversality conditions imply

$$\lambda_c(T) = \lambda_p(T) = 0. \quad (7)$$

It follows that $\lambda^0 < 0$. Indeed, if $\lambda^0 = 0$, the solution of (6) satisfying the transversality condition would satisfy $\lambda_c \equiv 0$ and $\lambda_p \equiv 0$. This gives us a contradiction because the pair (λ, λ^0) must be non-zero. By homogeneity of the Hamiltonian, we may then assume that $\lambda^0 = -1$. The Hamiltonian condition in Pontryagin's Principle then gives

$$u(t) \in \operatorname{argmax}_{v \in [0, 1]} H(x(t), \lambda(t), -1, v) \quad \text{a.e. } t \in [0, T]. \quad (8)$$

An extremal is a triplet $(x(\cdot), \lambda(\cdot), u(\cdot))$ satisfying (2)-(6)-(8) (since $\lambda^0 \neq 0$, we thus only consider normal extremals in the sequel). From (8), the control law is given by the sign of the *switching function*

$$\phi := \lambda_p k_R c(1 - c - p),$$

which gives

$$\begin{cases} \phi(t) > 0 &\Rightarrow u(t) = 1, \\ \phi(t) < 0 &\Rightarrow u(t) = 0. \end{cases} \quad (9)$$

A Bang+ arc (resp. Bang-) is a portion of trajectory defined over some time interval $[t_1, t_2]$ such that $u = +1$ (resp. $u = 0$) over $[t_1, t_2]$. The next property shows that any optimal control is necessarily of type Bang+ in some neighborhood of $t = T$.

Proposition 2. *If u is an optimal control of (P), there exists $\tau \in [0, T)$ such that one has $u(t) = +1$ for every $t \in [\tau, T]$.*

Proof. At time $t = T$, one has $\phi(T) = 0$. In addition, by differentiating ϕ w.r.t. t we find

$$\dot{\phi}(T) = -k_R c(T)(1 - c(T) - p(T))v'_P(p(T)) < 0$$

using $\lambda_c(T) = \lambda_p(T) = 0$. By continuity, there exists $\tau \in [0, T)$ such that one has $\phi > 0$ over $[\tau, T)$ implying the desired property. \square

The switching function ϕ may also vanish over a sub-interval $[t_1, t_2] \subset [0, T]$. If this happens, we say that the extremal is *singular* over $[t_1, t_2]$ and that a singular arc occurs. The singular arc is the portion of the corresponding trajectory over $[t_1, t_2]$. As we shall next see, such arcs have a significant impact on the optimal synthesis, that is why, we now study more into details their properties.

4.2 Study of singular arcs

In this section, we provide properties of singular arcs such as Legendre-Clebsch's condition that will allow us to have an insight into optimal paths. Recall that, given an optimal trajectory $(c(\cdot), p(\cdot))$ associated with a control $u(\cdot)$, along any singular arc defined over a time interval $[t_1, t_2]$, the inequality

$$\frac{\partial}{\partial u} \frac{d^2 H_u}{dt^2} \geq 0 \quad (10)$$

should be fulfilled over $[t_1, t_2]$. Inequality (10) expresses the second order necessary optimality condition (Legendre-Clebsch's condition). In particular, if (10) fails to hold, no singular arc occurs. In order to check if (10) is fulfilled, note that $\frac{\partial}{\partial u} \frac{d^2 H_u}{dt^2}$ coincides with $\ddot{\phi}|_u := \frac{\partial}{\partial u} \ddot{\phi}$.

Lemma 3. *Along any singular arc defined over a time interval $[t_1, t_2]$, one has:*

$$\lambda_c = \frac{-v'_P(p)}{k_R c + v'_P(p)(1 - c)} \text{ and } \dot{\lambda}_c = \frac{-v'_P(p)(v_P(p) + k_R(1 - 2c - p))}{k_R c + v'_P(p)(1 - c)}. \quad (11)$$

Proof. Along a singular arc defined over a time interval $[t_1, t_2]$, one has $\phi \equiv 0$ over $[t_1, t_2]$, thus $\lambda_p \equiv 0$ as well as $\dot{\lambda}_p \equiv 0$. By differentiating λ_p and using (6), we find the desired expressions of λ_c as well as $\dot{\lambda}_c$ along $[t_1, t_2]$. \square

Proposition 3. *Along any singular arc defined over a time interval $[t_1, t_2]$, the Legendre-Clebsch condition (10) is fulfilled with a strict inequality.*

Proof. Recall that along a singular arc $\lambda_p \equiv 0$. By differentiating ϕ w.r.t. t over $[t_1, t_2]$, we thus get

$$\dot{\phi} = -k_R c(1 - c - p)(k_R c \lambda_c + v'_P(p)(1 - c) \lambda_c + v'_P(p)).$$

Now, when differentiating $\dot{\phi}$ w.r.t. t , the terms involving explicitly the control u come from the derivate of the function $t \mapsto v'_P(p(t))$ w.r.t. t . Hence, along a singular arc, we find that

$$\begin{aligned} \ddot{\phi}|_u &= -k_R c(1 - c - p)v''_P(p)((1 - c)\lambda_c + 1)\dot{p}|_u \\ &= -\frac{k_R^2 c^2(1 - c - p)v''_P(p)}{k_R c + v'_P(p)(1 - c)}\dot{p}|_u \\ &= -\frac{k_R^3 c^3(1 - c - p)^2 v''_P(p)}{k_R c + v'_P(p)(1 - c)}, \end{aligned}$$

where the second equality follows from (11). Observe that the quantity $k_R c + v'_P(p)(1 - c)$ is positive. Since v_P is strictly concave, $v'_P < 0$, and we deduce that $\ddot{\phi}|_u > 0$. The result follows. \square

Remark 1. (i) *The fact that Legendre-Clebsch's condition is fulfilled indicates that the optimal synthesis may exhibit a singular arc (although the occurrence of such an arc also depends on the initial condition). If a singular arc occurs, such an arc is usually called a turnpike (see, e.g., [6] or [3]) meaning that during a certain time interval, the optimal control must take intermediate values between 0 and 1 (see Proposition 4). According to turnpike properties (see [39] and references herein), the corresponding portion of trajectory should then remain close to an optimal steady state point as computed in Section 3.*

(ii) Note also that the strict concavity of v_P is fundamental to ensure Legendre-Clebsch's condition : if $v_P'' = 0$, then $\dot{\phi}|_u$ would be zero implying the possible occurrence of a singular arc of second order (see [22]), i.e., the singular control cannot be computed from $\ddot{\phi}$ (as in Proposition 4), but from $\ddot{\phi}$.

We now provide the expression of the singular control as a feedback of the state.

Proposition 4. *Along a singular arc defined over a time interval $[t_1, t_2]$, the singular control $t \mapsto u_s(t)$ is given by $u_s(t) := \psi(c(t), p(t))$, $t \in [t_1, t_2]$ where $\psi : \Omega \rightarrow \mathbb{R}$ is defined as*

$$\psi(c, p) := -\frac{a(c, p)}{b(c, p)},$$

with

$$\begin{aligned} a(c, p) &:= -k_R (c p v_P(p) v_P''(p) + v_P'(p) [v_P'(p) ((1-c)^2 - p) + v_P(p) - k_R c^2]), \\ b(c, p) &:= k_R^2 c^2 (1-c-p) v_P''(p). \end{aligned} \quad (12)$$

Proof. Since $\lambda_p = \dot{\lambda}_p = 0$ over $[t_1, t_2]$, we find that

$$\begin{aligned} \ddot{\phi} &= k_R c (1-c-p) \ddot{\lambda}_p \\ &= -k_R c (1-c-p) \left[\dot{\lambda}_c [v_P'(p)(1-c) + k_R c] + \lambda_c \frac{d}{dt} [v_P'(p)(1-c) + k_R c] + v_P''(p) \dot{p} \right] \end{aligned} \quad (13)$$

Now, putting (11) into the previous expression and collecting the terms with u (coming from \dot{p}) and the ones without u allows to write (13) as

$$\ddot{\phi} = -\frac{k_R c (1-c-p)}{k_R c + v_P'(p)(1-c)} (a(c, p) + b(c, p)u),$$

where a, b are given by (12). Using that $\ddot{\phi} = 0$ over $[t_1, t_2]$, the result follows. \square

Remark 2. *To complete the sign condition (9) coming from the Hamiltonian condition (8), the previous proposition implies that if $\phi \equiv 0$ over some time interval $[t_1, t_2]$, then the corresponding singular path necessarily coincides with a portion of orbit of*

$$\begin{cases} \dot{c} &= v_P(p)(1-c) - k_R c(1-c-p), \\ \dot{p} &= -\frac{a(c, p)}{b(c, p)} k_R c(1-c-p) - p v_P(p), \end{cases} \quad (14)$$

that is, system (2) in which the input u is the feedback control $u = \psi(c, p)$.

We now analyze the asymptotic behavior of the dynamical system (14) near (c^*, p^*) .

Proposition 5. *The optimal steady-state point (c^*, p^*) is a saddle point of (14).*

Proof. First, note that system (14) can be equivalently rewritten

$$\begin{cases} \dot{c} &= v_P(p)(1-c) - k_R c(1-c-p), \\ \dot{p} &= \frac{v_P'(p)}{c v_P''(p)} (v_P'(p) [(1-c)^2 - p] + v_P(p) - k_R c^2) \end{cases} \quad (15)$$

Recall that the optimal steady-state point satisfies $p^* = (u^*)^2 = (1-c^*)^2$, $c^* = 1-u^*$ where u^* is the unique solution of the equation $v_P(u^2) = k_R(1-u^2)$ over $[0, 1]$. Thanks to these relations, we can verify that (c^*, p^*) is an equilibrium of (15). In addition, the Jacobian matrix of (15) at this point writes

$$A := \begin{bmatrix} \alpha & \beta \\ \gamma & \delta \end{bmatrix},$$

with

$$\begin{cases} \alpha &= -v_P(p^*) - k_R(1-2c^*-p^*), \\ \beta &= v_P'(p^*)(1-c^*) + k_R c^*, \\ \gamma &= -\frac{2v_P'(p^*)}{c^* v_P''(p^*)} (v_P'(p^*)(1-c^*) + k_R c^*), \\ \delta &= -\frac{v_P'(p^*)}{c^*} ((1-c^*)^2 - p^*). \end{cases}$$

We see that $\beta > 0$ and that $\gamma < 0$, and thanks to the definition of (c^*, p^*) , we verify that $\alpha = \delta = 0$. It follows that the matrix A has exactly two non-zero eigenvalues of opposite sign which ends the proof. \square

At this step, we have seen that an optimal control satisfies almost everywhere over $[0, T]$: either $u \in \{0, 1\}$ (depending on the sign of ϕ), or u is singular and its expression u_s is provided by Proposition 4. Observe that there is no guarantee that along a singular arc, the singular arc is *admissible*, i.e.,

$$|u_s| \leq 1. \quad (16)$$

Indeed, the value of the singular control $u_s = \psi(c, p)$ provided by the Pontryagin Maximum Principle may exceed the bounds on the control u . Nevertheless, when the singular arc is close to the optimal steady-state point, then inequality (16) is fulfilled as we shall next see.

Property 1. *There exists a neighborhood $\mathcal{V} \subset \Omega$ of (c^*, p^*) such that one has $|\psi(c, p)| \leq 1$ for every $(c, p) \in \mathcal{V}$.*

Proof. When $(c, p) \rightarrow (c^*, p^*)$, one has

$$\psi(c, p) \sim -\frac{k_R c^* p^* v_P(p^*) v_P''(p^*)}{k_R^2 (c^*)^2 (1 - c^* - p^*) v_P''(p^*)} = -\frac{p^* k_R (c^*)^2}{k_R c^* (1 - c^* - p^*)}$$

using that $v_P(p^*) = k_R (c^*)^2$ in the above equality. This gives

$$|\psi(c, p)| \sim \frac{c^* p^*}{1 - c^* - p^*} = 1 - c^*,$$

using $p^* = (1 - c^*)^2$ and the result follows since $c^* \in (0, 1)$. \square

So, we can conclude about the admissibility of a singular arc when the corresponding trajectory is sufficiently close to the saddle point (c^*, p^*) .

4.3 Discussion about optimal trajectories

The saddle point property of (c^*, p^*) along the singular arcs crucial in order to understand the behavior of optimal paths and it is in line with properties of turnpikes as in [39]. The optimal point (c^*, p^*) possesses a stable and unstable one-dimensional manifold. Hence, an optimal trajectory can take advantage of the stable manifold to approach (c^*, p^*) which by definition is the point for which production is optimal at steady-state. Because of the transversality conditions (recall that on optimal path contains a Bang + arc over some time interval $[T - \varepsilon, T]$), an optimal trajectory will leave a neighborhood of (c^*, p^*) taking advantage of the unstable manifold before switching to $u = +1$ until the terminal time.

Thanks to these qualitative properties, we can expect an optimal path to be of the following type:

$$\gamma_1 - \gamma_s - \gamma_2, \quad (17)$$

where γ_s is a singular arc, and $\gamma_i, i = 1, 2$ is the union of (possibly a few) Bang arcs.

- The first part γ_1 allows an optimal path to approach \mathcal{V} before switching to a singular arc.
- Along the singular arc γ_s , the trajectory stays close to the optimal steady-state.
- In the third part γ_2 , the trajectory moves away from the optimal steady-state point. For our biological problem, this last transient corresponds to an artifact due to a fixed final time (recall (7)), and only the transition from the initial condition to the optimal steady-state is relevant.

4.4 Numerical optimal solutions

In this section, we solve numerically the optimal control problem (P) by a direct method using the software `bocop` [38, 5]. This will corroborate the structure of an optimal control given by (17). A time discretization allows to transform the optimal control problem into a nonlinear optimization problem, solved here by interior point techniques. A discretization by a Lobatto IIIIC formula (6th order) was used with 400 time steps, and the relative tolerance for NLP solver was set at 10^{-10} .

The optimal trajectories obtained numerically are composed of two bang arcs followed by a singular arc (which approaches the optimal steady state), see Fig. 3.

These numerical results tend to confirm our conjecture about the structure of an optimal solution given by (17) : the optimal strategy corresponds to a turnpike behavior. Additionally, these results show the reliability of the numerical method. Trajectories are actually computed by the direct method, without any knowledge of the theoretical solution, and the numerical solutions present several characteristics demonstrated previously, such as the singular arc approaching to the optimal steady state (see Fig. 4).

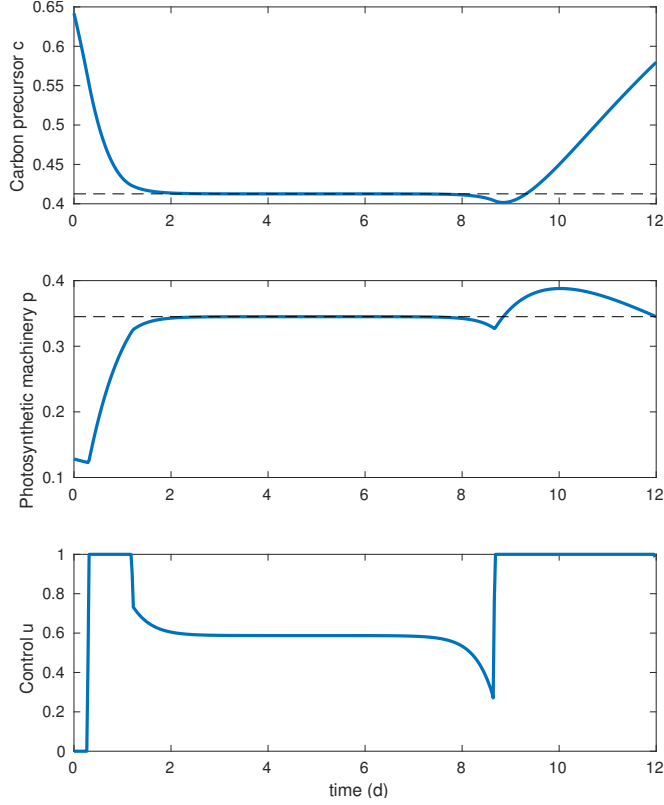


Figure 3: Optimal trajectory (solution of (P)), obtained numerically by the direct method using the `bocop` solver [38]. The black dashed lines correspond to the optimal steady-state.

5 Model fitting: a bi-level optimization problem

Several microbial models with dynamic resource allocation have been proposed recently, but comparison with experimental data is rarely carried out. In this context, we propose a numerical method to estimate model parameters from experimental data and finally evaluate if our framework allows to represent quantitatively microalgal photoacclimation dynamics. A light down-shift is used as a case study. After a long acclimation to a light intensity I^- , microalgae are shifted at $t = 0$ to a different intensity I .

5.1 Problem formulation

The model outputs y is a function g of the states $x = (c, p)$ and also possibly of the parameters θ , *i.e.*

$$y(t) = g(x(t), \theta),$$

We consider a set of measurements $\bar{y}_k \in \mathbb{R}^m$, corresponding to time instants t_1, \dots, t_{n_k} , $k \geq 1$. Our objective is to find the set of parameters $\theta = (k_P, k_R, K)^T \in (0, +\infty)^3$ such that the optimal solution $x(\cdot)$ of (P) fits the experimental data. This leads to a so-called *bi-level optimization problem*:

$$\begin{aligned} \min_{\theta \in C} & \sum_k (g(x^*(t_k), \theta) - \bar{y}_k)^T Q (g(x^*(t_k), \theta) - \bar{y}_k) \\ \text{s.t.} & \begin{cases} u^* & \in \operatorname{argmax}_{u \in \mathcal{U}} \int_0^T v_P(p(t)) dt, \\ \dot{x}(t) & = f(x(t), u(t), \theta) \quad \text{a.e. } t \in [0, T], \\ x(0) & = x^*(I^-, \theta), \end{cases} \end{aligned} \quad (18)$$

where $Q \in \mathcal{M}_{n_k}(\mathbb{R})$ is a square weighting matrix, C is a non-empty compact subset of $(0, +\infty)^3$, $f(\cdot, \cdot, \cdot)$ is the dynamics given by System (2) (in which we incorporate the dependency w.r.t. the parameters), x^* is the

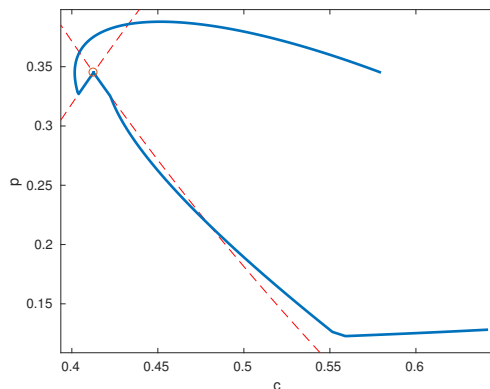


Figure 4: Plot of an optimal path (blue line) in the plane (c, p) by the direct method : in the first phase, the trajectory approaches (c^*, p^*) (red dot) ; in the second one, it remains close to it along a singular arc (red dashed lines) ; to satisfy transversality conditions it finishes with a single Bang+ arc.

solution to this system associated with $u^* \in \mathcal{U}$. In addition, the initial condition is $x^*(I^-, \theta)$ which is the optimal steady-state point as computed in Lemma 2, and which depends on the light intensity and parameters. Problem (P) plays the role of *lower level program* whereas the optimization w.r.t. θ in (18) is the *upper level program*. Problem (18) is unusual because it couples an optimal control problem to a non-linear program.

Experimental data with the microalga *Dunaliella tertiolecta* [34] have been considered. After several days of acclimation at $700 \mu\text{mol.m}^{-2}.\text{s}^{-1}$, light intensity has been shifted down to $70 \mu\text{mol.m}^{-2}.\text{s}^{-1}$ at $t = 0$. The following measurements have been used for parameter estimation:

- The relative content of LHCII, determined from Western blots. We consider that the photosynthetic sector p follows the same relative dynamics as this protein, and we fix arbitrarily the initial condition $p(0) = 0.1$.
- The photosynthetic rate (v_P), given in mole C.cell $^{-1}.\text{s}^{-1}$ and converted in d^{-1} assuming a carbon content of $3.5 \text{ pmole C.cell}^{-1}$ (determined by equilibrium values at low light).
- The cellular specific growth rate, which we assume corresponds to $v_R/(p + r)$, *i.e.*, the macromolecule synthesis rate per unit of macromolecule.

5.2 Numerical method

The solution of the bi-level optimization problem (18) is determined using a classical direct search routine (by the Levenberg-Marquardt method with the `lmfit` package in Python [26]). At each iteration, the `bocop` solver is called to solve the lower level problem for a given θ , using as initial condition the optimal steady-state (which depends on θ) for the light intensity of pre-acclimation. We take 100 time steps, with a time horizon large enough such that the second chattering arc occurs after the last measurement (this final arc is not relevant in our biological problem). For each variable, the square errors between the measurements and the optimal trajectory are weighted by the inverse of the square of the measurement mean. The computation time to solve the bi-level optimization problem on a classical laptop was approximatively one minute.

To better assess parameter uncertainty, pairwise confidence regions have been plotted using the function `conf_interval2d` from the `lmfit` package [26]. To do so, the two parameters for which the confidence region is calculated will be varied, while the remaining parameter is re-optimized. The fitting error is then used to evaluate the parameter confidence regions.

5.3 Fitting results

The estimated parameters with their confidence interval are given in Table 1. The optimal trajectory is shown with the experimental data in Fig. 5. The fitted optimal trajectory represents well the dynamics of photoacclimation. The photosynthetic rate falls sharply at $t = 0$ with the light down-shift, and then slowly

Table 1: Parameters (with their confidence intervals) estimated as the solution of the bi-level optimization problem (18)

Parameter	Definition	Value	Unit
k_P	Maximum photosynthetic rate	1.56 ± 0.26	d^{-1}
k_R	Macromolecule synthesis rate constant	2.11 ± 0.15	d^{-1}
K	Half saturation constant for photosynthesis	79.6 ± 21.2	$\mu\text{mol.m}^{-2}.\text{s}^{-1}$

increases with the reallocation of resources to the photosynthetic sector. On the other hand, the cellular growth rate (reflecting macromolecule synthesis) slowly decreases after the light shift, until reaching the new steady-state. The good model fit is the first hint that our approach is effective, and it should now be validated with other experiments. In Fig. 6, the parameter confidence regions show that k_p and K - the two parameters defining the photosynthetic rate - are correlated. More experimental data would be necessary to better estimate these parameters.

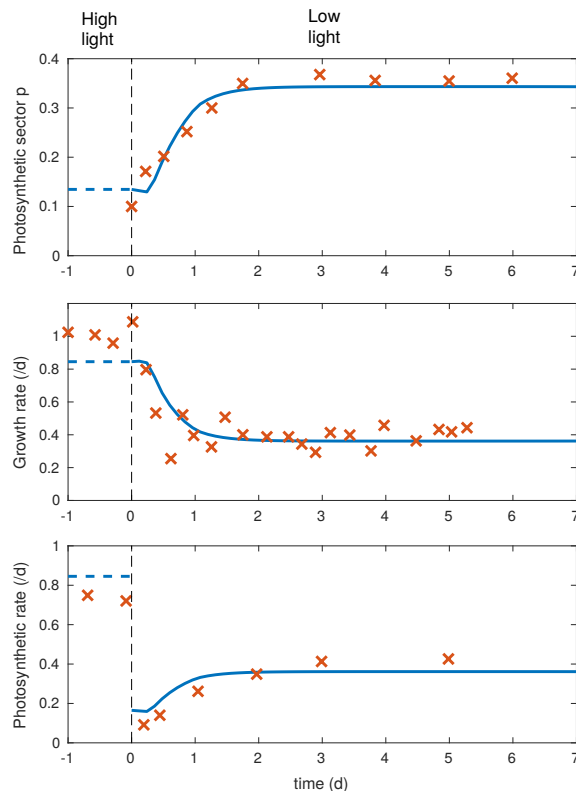


Figure 5: Trajectory corresponding to the solution of the bi-level optimization problem (18). The model (blue lines) fits the experimental data (red crosses) of the microalga *Dunaliella tertiolecta* facing a light intensity down-shift from $700 \mu\text{mol.m}^{-2}.\text{s}^{-1}$ to $70 \mu\text{mol.m}^{-2}.\text{s}^{-1}$ at $t = 0$ [34].

6 Optimal allocation under day/night cycles

Given that microalgae have evolved under day-night cycles, one may assume that they have an optimal allocation strategy to deal with these conditions. In this context, we wish to determine with our coarse-grained model the optimal trajectory under such a day/night cycle, by imposing that the initial condition is equal to the final condition (the cycle can thus be repeated day after day). This gives the following optimal

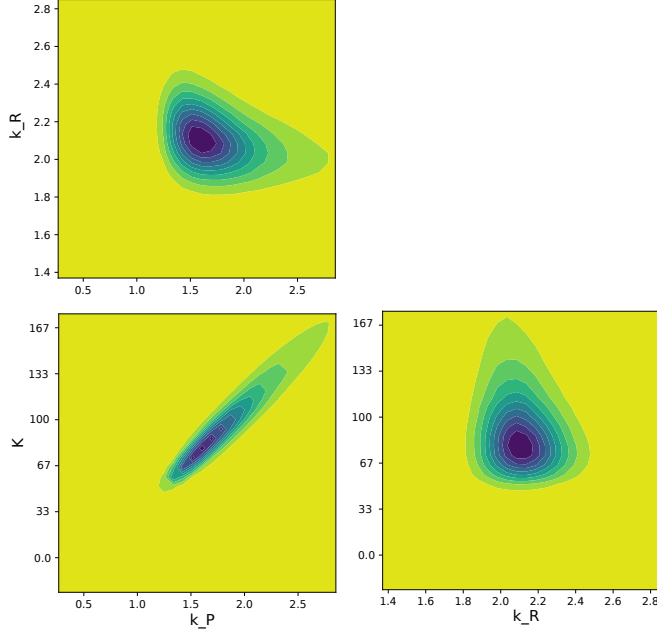


Figure 6: Pairwise confidence regions of model parameters, solution of the bi-level optimization problem (18). The two parameters k_p and K (which define the photosynthetic rate) are correlated.

periodic control problem:

$$\max_{u(\cdot) \in \mathcal{U}} J(u) := \int_0^T v_P(p(t), I(t)) dt, \quad \text{s.t. } (c(0), p(0)) = (c(T), p(T)), \quad (19)$$

where $(c(\cdot), p(\cdot))$ is the unique solution of (2) for a given control $u \in \mathcal{U}$, and $T = 1$ d. For the light pattern, we use a night period τ followed by a sinusoidal signal:

$$I(t) := \begin{cases} 0 & \text{for } 0 \leq t \leq \tau, \\ I_{\max} \sin^2\left(\frac{t-\tau}{T-\tau}\pi\right) & \text{for } \tau < t \leq T. \end{cases}$$

Note that in Problem (19), the initial condition is unknown since a periodic constraint on the state has been added.

Using our fitted model, optimal allocation strategy under day/night cycles is determined numerically using the direct method with `bocop` (as done previously in Section 4). In line with [18], we use $I_{\max} = 1000 \mu\text{mol}\cdot\text{m}^{-2}\cdot\text{s}^{-1}$ and $\tau = 0.41$ d. Results are presented in Fig. 7. The optimal trajectory consists in three Bang arcs, with the control u equals to 0-1-0. Note that several simulations with different parameter values and light signals (changing the maximum light intensity and the day length) have been carried out, and the structure of the optimal trajectory remains the same. Interestingly, the synthesis of the photosynthetic apparatus always begins a few hours before dawn in our predictions. This behavior is actually observed in several laboratory and field studies, see *e.g.*, [44, 20, 18]. Microalgae show thus an anticipation capacity - based a priori on their circadian clock [24, 36] - which allows them to deal with the day/night cycle optimally according to our assumptions.

7 Discussion

A coarse-grained model was proposed to predict microalgae growth and photoacclimation dynamics. Based on evolutionary principle, growth can be represented by an optimization problem: intracellular resources should be allocated in order to maximize microalgae growth over a time period. The optimal control problem was first studied with the Pontryagin Maximum Principle. Facing a light shift, we have shown that the optimal strategy of photoacclimation is a turnpike: after a transient, the trajectory remains close to the optimal steady

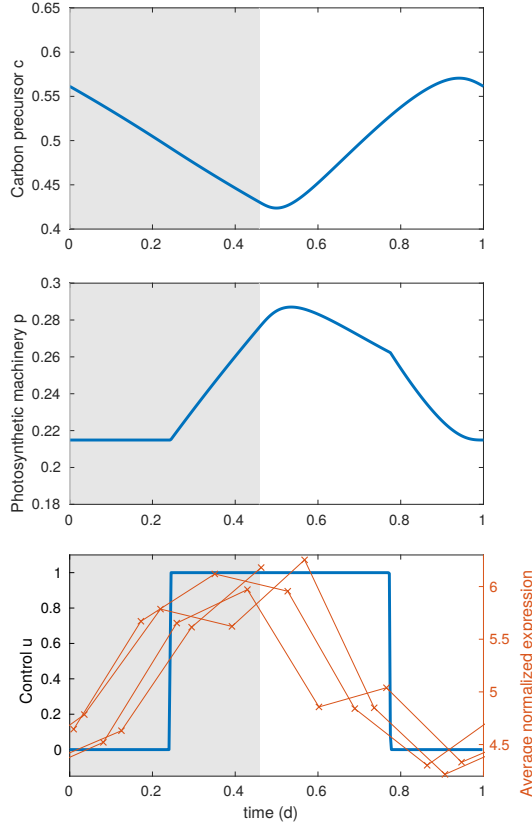


Figure 7: Optimal trajectory obtained numerically by the direct method using the bocop solver under day-night cycle. The control u (bottom figure, blue line, left axis), corresponding to the allocation of macromolecule synthesis to the photosynthetic apparatus, is switched on a few hours before dawn. This anticipatory behavior is in line with the averaged normalized expression of genes involved in photosynthesis in *Emiliana huxleyi* in the North Pacific Subtropical Gyre [18] (bottom figure, red marks, right axis).

state. Numerical results were in line with our analysis, confirming our development and the reliability of the numerical method. Model parameters were then estimated by solving a bi-level optimization problem. The model fits well photoacclimation dynamics when microalgae face a light down-shift. More surprising, the model also represents - at least qualitatively - the anticipation behavior of microalgae under day-night cycle: the synthesis of the photosynthetic apparatus starts a few hours before dawn, as observed experimentally in laboratory and field studies [44, 20, 18].

Several photoacclimation models have been proposed, where the allocation to the photosynthetic apparatus is either empiric (*i.e.*, defined as a function of environmental conditions) [13, 12, 4, 27, 33] or based on optimization principle [31, 2, 14, 19, 10, 43]. But, to our knowledge, only our approach allows to represent the anticipatory behavior of algae.

More generally, the anticipation capacity of microorganisms have been observed, *e.g.* in the bacteria *Escherichia coli* and the yeast *Saccharomyces cerevisiae* [23]. To represent anticipatory behavior with optimization-based models, optimization over a time window is necessary given that the biological response starts before the environmental signal. A notable example of cellular anticipation was proposed by [41] who predicted a change of gene expression before the complete depletion of a nutrient. On the other hand, anticipation is possible only in some conditions, *e.g.*, under periodic regime or if a signal announces a change of environmental conditions, and only if the species have evolved in these conditions. In consequence, optimization over a time period could not be used in any cases.

On a methodological aspect, the originality of this work is to propose a fitting procedure for dynamic resource allocation models, leading to a bi-level optimization problem in which the lower level is an optimal control problem and the upper one is a standard non-linear program.

A few studies have deal with this kind of problem, in particular to estimate the objective function that

a biological system optimizes (the so-called inverse optimal control problem). The cost function is generally written as a weighted sum of known functions, and the objective is thus to estimate the weights (leading to a parameter estimation problem). Such a problematic has been encountered in the context of motion planning. For instance, [25] have identified the underlying optimality criteria of human locomotion. The solution was obtained with two optimization algorithms, where the upper level calls at each iteration the lower level. In [1], a bilevel problem was also formulated to tackle arm movement. It was solved numerically by a discretization method and the use of optimality conditions in non-linear programming.

Closer to our study, [40] have proposed a computational approach to solve inverse optimal control problem in systems biology. As a first step, the inputs and parameters (corresponding respectively to $u(t)$ and θ with our notation) are estimated by minimizing the error between measurements and model outputs. The resulting parameters are then used to compute the Pareto set of optimal control. Finally, the objective function is estimated such that the optimal trajectory corresponds to the observed dynamics. The major advantage of this approach is that there is no longer a bi-level optimization problem, but identifiability issues are nevertheless to be feared when estimating the input.

The numerical methods proposed here and in the aforementioned studies work on relatively small models (with a limited number of variables), but new developments will be required for bigger models (*i.e.*, for metabolic models at genome scale). Finding issues in a general setting to this kind of optimization problems could also be investigated in future works.

8 Acknowledgement

This research benefited from the support of the FMJH Program PGM0 and from the support to this program from EDF-THALES-ORANGE. We are grateful to Walid Djema for fruitful exchanges about singular arcs.

References

- [1] S. Albrecht, M. Leibold, and M. Ulbrich. A bilevel optimization approach to obtain optimal cost functions for human arm movements. *Numerical Algebra, Control and Optimization*, 2:105–127, 2012.
- [2] R. Armstrong. Optimality-based modeling of nitrogen allocation and photoacclimation in photosynthesis. *Deep Sea Research Part II: Topical Studies in Oceanography*, 53(5-7):513–531, 2006.
- [3] T. Bayen, O. Cots, and P. Gajardo. Analysis of an Optimal Control Problem Related to the Anaerobic Digestion Process. *J. Optim. Theory Appl.*, 178(2):627–659, 2018.
- [4] O. Bernard, F. Mairet, and B. Chachuat. Modelling of microalgae culture systems with applications to control and optimization. In *Microalgae Biotechnology*, pages 59–87. Springer, 2015.
- [5] J. Bonnans, Frederic, D. Giorgi, V. Grelard, B. Heymann, S. Maindrault, P. Martinon, O. Tissot, and J. Liu. Bocop A collection of examples. Technical report, INRIA, 2017.
- [6] U. Boscain and B. Piccoli. *Optimal syntheses for control systems on 2-D manifolds*, volume 43 of *Mathématiques & Applications (Berlin) [Mathematics & Applications]*. Springer-Verlag, Berlin, 2004.
- [7] L. Cesari. *Optimization - Theory and Applications. Problems with Ordinary Differential Equations*. Springer-Verlag, Applications of Mathematics, 17, 1983.
- [8] D. Cohen and H. Parnas. An optimal policy for the metabolism of storage materials in unicellular algae. *Journal of theoretical biology*, 56(1):1–18, 1976.
- [9] T. de Mooij, Z. R. Nejad, L. van Buren, R. H. Wijffels, and M. Janssen. Effect of photoacclimation on microalgae mass culture productivity. *Algal research*, 22:56–67, 2017.
- [10] M. Faizi and R. Steuer. Optimal proteome allocation strategies for phototrophic growth in a light-limited chemostat. *Microbial cell factories*, 18(1):165, 2019.
- [11] P. G. Falkowski and J. A. Raven. *Aquatic Photosynthesis*. Princeton University Press, Princeton, 2007.

- [12] F. García-Camacho, A. Sánchez-Mirón, E. Molina-Grima, F. Camacho-Rubio, and J. Merchuck. A mechanistic model of photosynthesis in microalgae including photoacclimation dynamics. *Journal of theoretical biology*, 304:1–15, 2012.
- [13] R. Geider, H. MacIntyre, and T. Kana. A dynamic regulatory model of phytoplankton acclimation to light, nutrients, and temperature. *Limnology and Oceanography*, pages 679–694, 1998.
- [14] R. J. Geider, C. M. Moore, and O. N. Ross. The role of cost–benefit analysis in models of phytoplankton growth and acclimation. *Plant Ecology & Diversity*, 2(2):165–178, 2009.
- [15] N. Giordano, F. Mairet, J.-L. Gouzé, J. Geiselman, and H. de Jong. Dynamical allocation of cellular resources as an optimal control problem: Novel insights into microbial growth strategies. *PLOS Computational Biology*, 12(3):e1004802, 2016.
- [16] J. R. Graff, T. K. Westberry, A. J. Milligan, M. B. Brown, G. D. Olmo, K. M. Reifel, and M. J. Behrenfeld. Photoacclimation of natural phytoplankton communities. *Marine Ecology Progress Series*, 542:51–62, 2016.
- [17] H. Havelková-Doušová, O. Prášil, and M. Behrenfeld. Photoacclimation of *Dunaliella tertiolecta* (chlorophyceae) under fluctuating irradiance. *Photosynthetica*, 42(2):273–281, 2004.
- [18] M. D. Hernández Limón, G. M. Hennon, M. J. Harke, K. R. Frischkorn, S. T. Haley, and S. T. Dyrman. Transcriptional patterns of *emiliania huxleyi* in the north pacific subtropical gyre reveal the daily rhythms of its metabolic potential. *Environmental Microbiology*, 22(1):381–396, 2020.
- [19] M. Jahn, V. Vialas, J. Karlsen, G. Maddalo, F. Edfors, B. Forsström, M. Uhlén, L. Käll, and E. P. Hudson. Growth of cyanobacteria is constrained by the abundance of light and carbon assimilation proteins. *Cell reports*, 25(2):478–486, 2018.
- [20] D. E. John, J. M. Lopez-Diaz, A. Cabrera, N. A. Santiago, J. E. Corredor, D. A. Bronk, and J. H. Paul. A day in the life in the dynamic marine environment: how nutrients shape diel patterns of phytoplankton photosynthesis and carbon fixation gene expression in the mississippi and orinoco river plumes. *Hydrobiologia*, 679(1):155–173, 2012.
- [21] H. MacIntyre, T. Kana, T. Anning, and R. Geider. Photoacclimation of photosynthesis irradiance response curves and photosynthetic pigments in microalgae and cyanobacteria. *J. Phycol.*, 38(1):17–38, 2002.
- [22] F. Mairet and T. Bayen. Parameter estimation for dynamic resource allocation in microorganisms: A bi-level optimization problem. In *Proceedings of the 21st IFAC World Congress*, 2020.
- [23] A. Mitchell, G. H. Romano, B. Groisman, A. Yona, E. Dekel, M. Kupiec, O. Dahan, and Y. Pilpel. Adaptive prediction of environmental changes by microorganisms. *Nature*, 460(7252):220–224, 2009.
- [24] M. Mittag. Circadian rhythms in microalgae. In *International review of cytology*, volume 206, pages 213–247. Elsevier, 2001.
- [25] K. Mombaur, A. Truong, and J.-P. Laumond. From human to humanoid locomotion an inverse optimal control approach. *Autonomous robots*, 28(3):369–383, 2010.
- [26] M. Newville, T. Stensitzki, D. B. Allen, and A. Ingargiola. LMFIT: Non-Linear Least-Square Minimization and Curve-Fitting for Python, Sept. 2014.
- [27] A. Nikolaou, P. Hartmann, A. Sciandra, B. Chachuat, and O. Bernard. Dynamic coupling of photoacclimation and photoinhibition in a model of microalgae growth. *Journal of theoretical biology*, 390:61–72, 2016.
- [28] M. Y. Pavlov and M. Ehrenberg. Optimal control of gene expression for fast proteome adaptation to environmental change. *Proceedings of the National Academy of Sciences*, 110(51):20527–20532, 2013.
- [29] L. Pontryagin, V. Boltyanskiy, R. Gamkrelidze, and E. Mishchenko. *Mathematical theory of optimal processes*. New York, 1964.

- [30] A.-M. Reimers, H. Knoop, A. Bockmayr, and R. Steuer. Cellular trade-offs and optimal resource allocation during cyanobacterial diurnal growth. *PNAS*, 114(31):E6457–E6465, 2017.
- [31] B. Shuter. A model of physiological adaptation in unicellular algae. *Journal of theoretical biology*, 78(4):519–552, 1979.
- [32] P. Spolaore, C. Joannis-Cassan, E. Duran, and A. Isambert. Commercial applications of microalgae. *Journal of bioscience and bioengineering*, 101(2):87–96, 2006.
- [33] L. Straka and B. E. Rittmann. Light-dependent kinetic model for microalgae experiencing photoacclimation, photodamage, and photodamage repair. *Algal research*, 31:232–238, 2018.
- [34] A. Sukenik, J. Bennett, A. Mortain-Bertrand, and P. G. Falkowski. Adaptation of the photosynthetic apparatus to irradiance in *Dunaliella tertiolecta*: a kinetic study. *Plant physiology*, 92(4):891–898, 1990.
- [35] W. J. Sutherland. The best solution. *Nature*, 435(7042):569–569, 2005.
- [36] L. Suzuki and C. H. Johnson. Algae know the time of day: circadian and photoperiodic programs. *Journal of Phycology*, 37(6):933–942, 2001.
- [37] D. Talmy, J. Blackford, N. J. Hardman-Mountford, A. J. Dumbrell, and R. J. Geider. An optimality model of photoadaptation in contrasting aquatic light regimes. *Limnology and oceanography*, 58(5):1802–1818, 2013.
- [38] Team Commands, Inria Saclay. Bocop: an open source toolbox for optimal control. <http://bocop.org>, 2017.
- [39] E. Trélat and E. Zuazua. The turnpike property in finite-dimensional nonlinear optimal control. *Journal of Differential Equations*, 258(1):81–114, 2015.
- [40] N. Tsiantis, E. Balsa-Canto, and J. R. Banga. Optimality and identification of dynamic models in systems biology: an inverse optimal control framework. *Bioinformatics*, 34(14):2433–2440, 2018.
- [41] S. Waldherr, D. A. Oyarzún, and A. Bockmayr. Dynamic optimization of metabolic networks coupled with gene expression. *Journal of theoretical biology*, 365:469–485, 2015.
- [42] K. W. Wirtz and M. Pahlow. Dynamic chlorophyll and nitrogen: carbon regulation in algae optimizes instantaneous growth rate. *Marine Ecology Progress Series*, 402:81–96, 2010.
- [43] T. Závřel, M. Faizi, C. Loureiro, G. Poschmann, K. Stühler, M. Sinetova, A. Zorina, R. Steuer, and J. Červený. Quantitative insights into the cyanobacterial cell economy. *eLife*, 8:e42508, 2019.
- [44] E. R. Zinser, D. Lindell, Z. I. Johnson, M. E. Futschik, C. Steglich, M. L. Coleman, M. A. Wright, T. Rector, R. Steen, N. McNulty, et al. Choreography of the transcriptome, photophysiology, and cell cycle of a minimal photoautotroph, prochlorococcus. *PloS one*, 4(4):e5135, 2009.